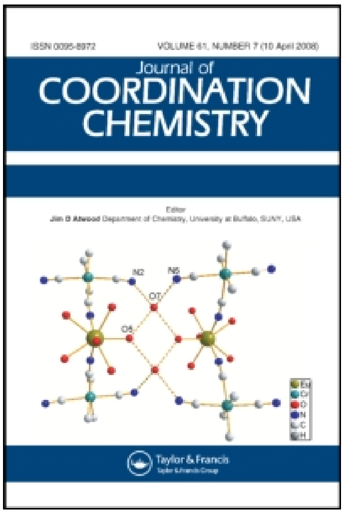

Journal of Coordination Chemistry
Publication details, including instructions for authors and subscription information:
http://www.informaworld.com/smpp/title~content=t713455674

A new oxamato-bridged heterotrinuclear $Ni^{II}Cu^{II}Ni^{II}$ complex: synthesis, structure and properties

Yong-Sheng Yang[a]; Wen Gu[a]; Li-Zhi Zhang[a]; Feng-Xian Gao[a]; Shi-Ping Yan[a]
[a] Department of Chemistry, Nankai University, 300071 Tianjin, P.R. China

To cite this Article Yang, Yong-Sheng , Gu, Wen , Zhang, Li-Zhi , Gao, Feng-Xian and Yan, Shi-Ping(2008) 'A new oxamato-bridged heterotrinuclear $Ni^{II}Cu^{II}Ni^{II}$ complex: synthesis, structure and properties', Journal of Coordination Chemistry, 61: 4, 571 — 578

To link to this Article: DOI: 10.1080/00958970701364842

URL: http://dx.doi.org/10.1080/00958970701364842

Journal of Coordination Chemistry
Vol. 61, No. 4, 20 February 2008, 571–578

A new oxamato-bridged heterotrinuclear $Ni^{II}Cu^{II}Ni^{II}$ complex: synthesis, structure and properties

YONG-SHENG YANG, WEN GU, LI-ZHI ZHANG, FENG-XIAN GAO and SHI-PING YAN*

Department of Chemistry, Nankai University, 300071,
Tianjin, P.R. China

(*Received 4 January 2007; in final form 12 February 2007*)

A new oxamato-bridged $Ni^{II}Cu^{II}Ni^{II}$ species, $[Ni(iprtacn)]_2[Cu(pba)(H_2O)_{0.5}](BPh_4)_2$ (**1**), (iprtacn = 1,4,7-triisopropyl-1,4,7-triazacyclononane; pba = 1,3-propylenebis(oxamato)) has been synthesized and structurally as well as magnetically characterized. Complex **1** has a discrete trinuclear $Ni^{II}Cu^{II}Ni^{II}$ structure: Two nickel(II) ions are bridged by $[Cu(pba)]^{2-}$ with the macrocyclic ligand iprtacn a terminal ligand of nickel(II). Fitting the magnetic data of **1** led to $g_{Cu} = 2.16$, $g_{Ni} = 2.18$, $J = -112.5\,cm^{-1}$, $D = \pm 7.78\,cm^{-1}$. The irregular spin state structure and interaction of complex 1with DNA are described here.

Keywords: Heterotrinuclear $Ni^{II}Cu^{II}Ni^{II}$ complex; Magnetic properties; Irregular spin state; Interaction with DNA

1. Introduction

Molecular magnetism has had rapid development in the last few years [1–3]. One of the main challenges is the design of molecular ferromagnets; several approaches have been proposed [4–6]. Particular emphasis has been placed on heterobimetallic complexes, and much of this research has been directed toward transition metal clusters [7–11]. High-spin multiplicity in a polymetallic entity could be stabilized without imposing ferromagnetic interactions between the nearest magnetic centers [12–16]. To achieve this, two high local spins are aligned in the same direction due to antiferromagnetic interactions with a small spin located between them. The small central spin polarizes the two high terminal spins in a ferromagnetic-like fashion. In a linear trinuclear system ABA, when the A–B interaction is antiferromagnetic, the ground state does not have the lowest spin if $2S_A > S_B + 1/2$, which is the so called irregular spin state. This may lead to magnetic behavior with a minimum in the $\chi_M T$ *versus* T plot.

---

*Corresponding author. Email: yansp@nankai.edu.cn

Journal of Coordination Chemistry
ISSN 0095-8972 print/ISSN 1029-0389 online © 2008 Taylor & Francis
DOI: 10.1080/00958970701364842

Below the minimum, the compound exhibits ferromagnetic-like behavior. Irregular spin state has been achieved, for instance, in some $Ni^{II}Cu^{II}Ni^{II}$ [12–16], $Co^{II}Cu^{II}Co^{II}$ [17], $Mn^{II}Cu^{II}Mn^{II}$ [12–16, 18], and $Fe^{III}Ni^{II}Fe^{III}$ species [19]. To obtain the desired topology, chemists have to design and synthesize a species with a special molecular topology. In this paper, we reported the synthesis, magnetic and spectroscopic properties of a new oxamato-bridged $Ni^{II}Cu^{II}Ni^{II}$ species, $[Ni(iprtacn)]_2[Cu(pba)(H_2O)_{0.5}](BPh_4)_2$ (**1**). Interaction with DNA is also discussed here.

2. Experimental

2.1. *General remarks*

All the starting chemicals and solvents were of reagent grade and used as received without further purification. The copper(II) precursors $Na_2[Cu(pba)] \cdot 6H_2O$ [20], and macrocyclic ligand iprtacn [21], were prepared according to published procedures. Elemental analyses for C, H and N were carried out on a Model 240 Perkin–Elmer instrument. IR spectra were measured using KBr disks in a Bruker Tensor 27 FT-IR spectrophotometer in the 400–4000 cm^{-1} region. Electronic spectra were measured with a Jasci V-570 UV-Vis spectrophotometer in the 200–2000 nm region in aqueous solution. Variable-temperature magnetic susceptibility measurements were performed on a SQUID MPMS XL-7 magnetometer in an applied magnetic field of 1 KG. The experimental susceptibilities were corrected for diamagnetism of the constituent atoms (Pascal's tables) [22].

2.2. *Synthesis*

The species $iprtacnNiCl_2$ was synthesized acoording to the literature [10]. 0.0578 g (0.15 mmol) of $Ni(iPrtacn)Cl_2$ was dissolved in 20 mL of methanol, then 0.0326 g (0.075 mmol) of $Na_2[Cu(pba)] \cdot 6H_2O$ was added as solid to the nickel solution and stirred; after all the solid was dissolved, 0.0648 mg (0.15 mmol) of $NaBPh_4$ dissolved in 20 mL of methanol was added to the previous solution dropwise. A blue precipitate appeared, which was filtered, washed with methanol and dried under vacuum. Single crystals were obtained by slow evaporation of an acetone solution of the powder containing a small amount of CH_3CN. Yield of crystals 70%. Anal. Calcd for $C_{83}H_{113}B_2CuN_8Ni_2O_{6.5}$: C, 65.26; H, 7.18; N, 7.38. Found: C, 65.18; H, 7.45; N, 7.33%. Main IR bands (KBr, cm^{-1}): 3500–3200s (br), 3054s, 2979s, 1633vs, 1450s, 1397m, 1319m, 1230m, 1144s, 1063m, 961m, 735s, 705vs, 611m.

2.3. *Crystal structure determination and refinement*

A suitable crystal with dimension of $0.14 \times 0.12 \times 0.08\,mm^3$ for the complex was selected and mounted on a Bruker Smart 1000 diffractometer with graphite monochromated Mo-Kα radiation ($\lambda = 0.71070$ Å) at 293(2) K. Diffraction data were collected using $\omega - 2\theta$ scans at room temperature. LP correction was applied to the data. The structure was solved by direct methods using SHELXS-97 and refinement

Table 1. Crystal data and structure refinement for the complex.

Empirical formula	$C_{83}H_{113}B_2CuN_8Ni_2O_{6.5}$
Formula weight	1553.42
Temperature (K)	293(2)
Wavelength (Å)	0.71070
Crystal system, Space group	Monoclinic, $P2(1)/n$
Unit cell dimensions (Å, °)	
a	9.9140(19)
b	33.009(6)
c	14.156(3)
α	90
β	95.178(6)
γ	90
Volume ($Å^{-3}$)	4613.8(15)
Z, Calculated density ($Mg\,m^{-3}$)	4, 1.118
Absorption coefficient (mm^{-1})	0.683
$F(000)$	1652
Crystal size (mm^3)	$0.14 \times 0.12 \times 0.08$
θ range for data collection (°)	1.57 to 25.00
Limiting indices	$-11 \le h \le 11$, $-39 \le k \le 39$, $-16 \le l \le 16$
Reflections collected/unique	34581/8113
R(int)	0.0430
Max. and min. transmission	0.960 and 0.847
Data/restraints/parameters	8113/90/543
Goodness-of-fit on F^2	1.114
Final R indices $[I > 2\theta(I)]$	$R_1 = 0.0767$, $wR_2 = 0.2379$
R indices (all data)	$R_1 = 0.0881$, $wR_2 = 0.2502$
Largest diff. peak and hole ($e\,Å^{-3}$)	0.858 and −0.392

on F^2 was performed using SHELXL-97 by full-matrix least-squares procedure with anisotropic thermal parameters for all non-hydrogen atoms [23]. Hydrogen atoms were added theoretically and refined with riding model position parameters and isotropically refined. The crystal data and refinement details are summarized in table 1.

3. Results and discussion

3.1. *IR and electronic spectra*

IR spectra of **1** exhibit a broad medium band at ca 3100–3500 cm^{-1}, which may be assigned to the N–H group in iprtacn together with O–H group stretching mode absorption in H_2O molecules. The broad strong band between 1585 and 1634 cm^{-1} may be attributed to the $\nu_{c=o}$ vibrations of the oxamato group [24]. Additionally, abundant absorption peaks in the region 700–740 cm^{-1} strongly argues in favor of the presence of phenyl. The electronic absorption spectra of **1** were measured in aqueous solution. Complex **1** exhibits a very intense band at 268 nm, assignable to charge-transfer transitions in the Cu(II) chromophores and/or intraligand π–π* interactions. Moreover, in the visible region, complex **1** exhibits three broad bands: 621 nm ($\varepsilon = 110.7\,M^{-1}\,cm^{-1}$), 850 nm ($\varepsilon = 16.5\,M^{-1}\,cm^{-1}$), and 1187 nm ($\varepsilon = 30.7\,M^{-1}\,cm^{-1}$). The band at 621 nm can be attributed to the envelope of two spin allowed d–d transitions: $^2B_2(Cu) \rightarrow {}^2B_1(Cu)$ and $^3A_{2g}(Ni) \rightarrow {}^3T_{1g}(Ni)$. The band at 850 nm is due to

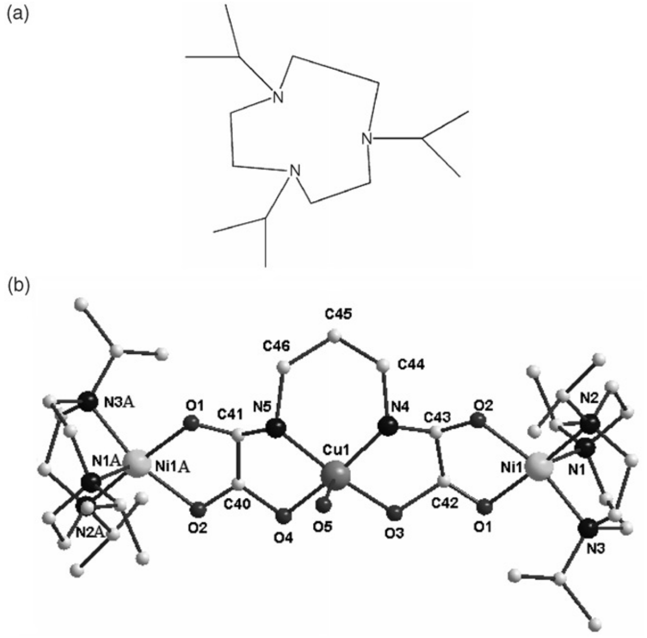

Figure 1. (a) The drawing of iprtacn. (b) Thermal ellipsoid diagram of $[Ni(iprtacn)]_2[Cu(pba) \cdot 0.5H_2O]^{2+}$.

$^3A_{2g}(Ni) \rightarrow {}^3T_{2g}(Ni)$ transition of Ni(II), assuming an O_h site symmetry for Ni(II). While the band at 1187 nm is attributable to the transition of $^3A_{2g}(Ni) \rightarrow {}^1E_g(Ni)$, which is activated by an exchange mechanism [25, 26].

3.2. *Description of the structure*

A drawing of ligand and perspective view of the title complex is shown in figure 1 and selected bond lengths and angles are listed in table 2. The complex, crystallized as $[Ni(iprtacn)]_2[Cu(pba)(H_2O)_{0.5}](BPh_4)_2$, belongs to the monoclinic system. Two Ni(II) atoms are bridged by $[Cu(pba)]^{2-}$ iprtacn is a terminal ligand of Ni(II). The BPh_4^- are counterions. The group $[Cu(pba)(H_2O)_{0.5}]$ is disordered, and the occupying probability of the water molecular is 50% coordinating to the Cu1 atom. The disorder on the group $[Cu(pba)(H_2O)_{0.5}]$ was modelled simply by refining and subsequently fixing the occupancy of the atoms. This atom had to be included in the refinement isotropically due to strong correlations between S.O.F. and displacement parameters. The Cu1(II) atom displays a slightly distorted square-pyramidal geometry, with the N(4), N(5), O(3), O(4) forming the basal plane and has an average distance of 2.151 Å to the Cu1 atom; O(5) occupies the axial position with a slightly longer distance of 2.356 Å. The deviation of Cu1 atom from the basal plane is 0.864 Å. Ni is five-coordinate, which is unique in $Ni^{II}Cu^{II}Ni^{II}$ system. Both terminal Ni(II) atoms are in a distorted square-pyramidal geometry. Their basal planes are formed by two nitrogen atoms (N(2), N(3)) from iprtacn and two oxygen atoms (O(1), O(2)) from the oxamato ligand. The axial position is provided by the other nitrogen atom (N(1)) from the iprtacn ligand

Table 2. Selected bond lengths (Å) and angles (°) for the complex.

Ni(1)–O(2)	2.009(3)	O(4)–Cu(1)	2.168(7)
Ni(1)–N(1)	2.049(4)	N(4)–Cu(1)	2.108(9)
Ni(1)–O(1)	2.051(3)	N(5)–Cu(1)	2.255(9)
Ni(1)–N(2)	2.087(3)	O(5)–Cu(1)	2.36(3)
O(3)–Cu(1)	2.071(8)		
O(2)–Ni(1)–N(1)	115.85(14)	C(42)–N(5)–Cu(1)	98.9(5)
O(2)–Ni(1)–O(1)	82.00(12)	C(46)–N(5)–Cu(1)	101.5(5)
N(1)–Ni(1)–O(1)	96.31(13)	O(3)–Cu(1)–N(4)	79.6(3)
O(2)–Ni(1)–N(3)	155.69(14)	O(3)–Cu(1)–O(4)	84.8(3)
N(1)–Ni(1)–N(3)	88.46(13)	N(4)–Cu(1)–O(4)	132.2(2)
O(1)–Ni(1)–N(3)	96.28(14)	O(3)–Cu(1)–N(5)	132.6(2)
O(2)–Ni(1)–N(2)	94.31(13)	N(4)–Cu(1)–N(5)	82.8(3)
N(1)–Ni(1)–N(2)	87.57(14)	O(4)–Cu(1)–N(5)	75.4(3)
O(1)–Ni(1)–N(2)	175.52(13)	O(3)–Cu(1)–O(5)	102.5(8)
N(3)–Ni(1)–N(2)	86.03(15)	N(4)–Cu(1)–O(5)	119.8(8)
C(40)–N(4)–Cu(1)	100.0(6)	O(4)–Cu(1)–O(5)	107.6(8)
C(44)–N(4)–Cu(1)	109.3(5)	N(5)–Cu(1)–O(5)	124.3(8)

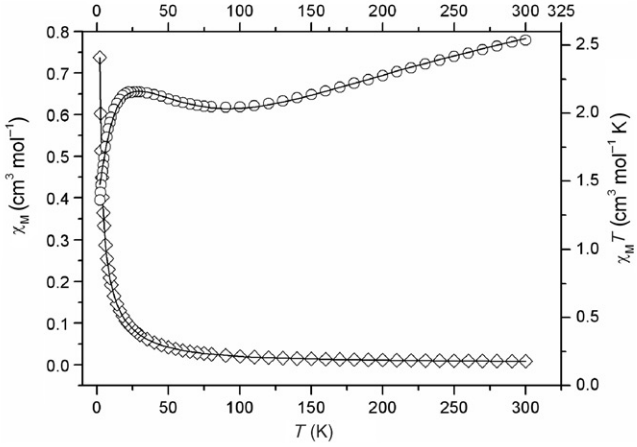

Figure 2. Experimental and calculated variations of χ_M (◇) and $\chi_M T$ (○) *vs.* T for complex **1**.

which adopts the *fac* conformation for the two Ni(II) ions. The Ni(1)–Cu(1)–Ni(1A) angle is 169.24°, and intramolecular separations between metal ions are Cu(1) ··· Ni(1) = 5.240 Å and Cu(1) ··· Ni(1A) = 5.234 Å, respectively, compatible with that of $\{[Ni(H_2O)(dpt)]_2[\mu\text{-}Cu(H_2O)(opba)]\}(ClO_4)_2 \cdot H_2O$ (Ni(1)–Cu(1)–Ni(2): 165.96°, Ni(1)–Cu(1): 5.347 Å, Cu(1)–Ni(2): 5.327 Å) [16].

3.3. *Magnetic properties*

The magnetic susceptibility of **1** was measured in the temperature range 2–300 K on a SQUID MPMS XL-7 magnetometer. The χ_M and $\chi_M T$ *versus* T plots are shown in figure 2. The room temperature value for $\chi_M T$ (2.54 $cm^3\,mol^{-1}$ K) is slightly higher than expected for spin only ($\chi_M T = 2.38\,cm^3\,mol^{-1}$ K). Upon cooling, the $\chi_M T$ value decreases smoothly reaching a minimum at ca 90 K ($\chi_M T = 2.04\,\mathrm{cm^3\,mol^{-1}\,K}$). Below 90 K, the $\chi_M T$ increases smoothly upon cooling further reaching a maximum with $\chi_M T = 2.16\,\mathrm{cm^3\,mol^{-1}\,K}$ at 28 K. After this maximum, the $\chi_M T$ value decreases slightly, with $\chi_M T = 1.36\,\mathrm{cm^3\,mol^{-1}\,K}$ at 2 K. The spin-state is irregular, that is, the energy of the low-lying states does not vary monotonically with spin. In the case in which the interaction between Ni(II) and Cu(II) is antiferromagnetic, the ground state is a quartet, above which there are two doublets, another quartet, and one sextuplet. Such magnetic behavior at low temperature may be attributed to the zero-field splitting within the quartet ground state. To simulate the experimental magnetic behavior, we used the following spin Hamiltonian that includes the ZFS parameter D of the ground state, where the ZFS is assumed to be axial for simplicity.

$$\hat{H} = -J(\hat{S}_{\mathrm{Ni1}} \cdot \hat{S}_{\mathrm{Cu}} + \hat{S}_{\mathrm{Ni1A}} \cdot \hat{S}_{\mathrm{Cu}}) + D\left[\hat{S}_Z^2 - \frac{1}{3}S(S+1)\right] + \beta[g_{\mathrm{Ni}}(\hat{S}_{\mathrm{Ni1}} + \hat{S}_{\mathrm{Ni1A}}) + g_{\mathrm{Cu}}\hat{S}_{\mathrm{Cu}}]H$$

The expression of the parallel and perpendicular magnetic susceptibility deduced from the Hamiltonian has already been shown described [13–15]. The increased $\chi_M T$ values at low temperatures can be due to weak ferromagnetic coupling between the trinuclear entities associated with structural parameters. Fitting the experimental data to the expression leads to the parameters $g_{\mathrm{Cu}} = 2.16$, $g_{\mathrm{Ni}} = 2.18$, $J = -112.5\,\mathrm{cm^{-1}}$, $D = \pm 7.78\,\mathrm{cm^{-1}}$, the agreement factor R $[R = \sum(\chi_{\mathrm{Obs}} - \chi_{\mathrm{Calcd}})^2/\sum(\chi_{\mathrm{Obs}})^2] = 2.74 \times 10^{-5}$. The magnetic properties are very similar with the complex $\{[\mathrm{Ni(cth)}]_2[\mu\text{-}\mathrm{Cu(Me_2pba)}]\}(\mathrm{ClO_4})_2$ ($g_{\mathrm{Cu}} = 2.10$, $g_{\mathrm{Ni}} = 2.13$, $J = -99.4\,\mathrm{cm^{-1}}$, $D = \pm 8.3\,\mathrm{cm^{-1}}$) [14].

3.4. *Spectroscopic discussion on DNA interaction*

In order to investigate whether DNA was the biological target of the compound, its interactions with Calf-thymus DNA (CT-DNA) were determined by UV-Vis and Fluorescence spectroscopy. The binding of copper ions to DNA is well established as is their ability to cleave DNA, particularly when Cu(II) ions are complexed with certain metal ion chelators. The concentration of CT-DNA per base was determined by recording the UV-Vis absorption at 260 nm using the molar absorption coefficient of $6600\,\mathrm{M^{-1}\,cm^{-1}}$. The UV-Vis absorbances at 260 and 280 nm of the CT-DNA solution in Tris-$\mathrm{Na_2EDTA}$ buffer gives a ratio of 1.87, indicating that the DNA was sufficiently free of protein. The concentration of the compound was 4.0×10^{-5} M. The fluorescence spectra were recorded at room temperature with excitation wavelength at 526 nm. The experiment was carried out by titrating the compound (4.0×10^{-3} M) into samples containing 1×10^{-4} M DNA and 2.5×10^{-5} M EB. The absorption spectra of the compound in the absence and presence of CT-DNA at various concentrations are given in figure 3. Free iprtacn does not have absorption in the ultraviolet region because of the high energy gap between LUMO and HOMO. However, nickel binding lowered the gap causing the transition at 257 nm. All bands showed hypochromism with increasing ratio of [DNA]/[compound], the LMCT band decreased about 40.5% in intensity when the ratio increased from 0.0 to 0.6. The DNA–EB system was used to further probe the DNA binding of the compound. Ethidium bromide (EB) is an intercalator that gives a

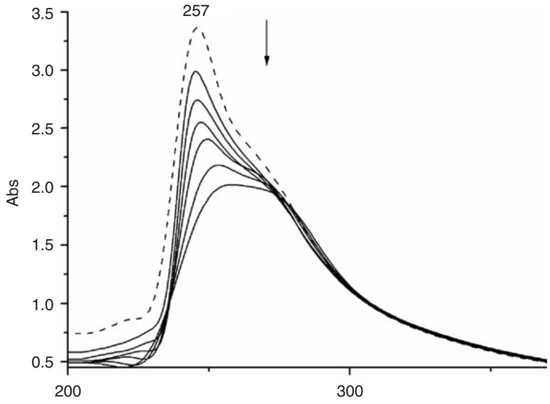

Figure 3. UV-Vis absorption spectra of the compound in 1 : 3 mixed solution of DMSO and Buffer (buffer = 10 mM tris, 1 mM Na_2EDTA, pH 7.50) with increasing concentration of CT-DNA. The concentration of the compound is 4.0×10^{-5} M, $r =$ [CT-DNA]/[compound] = 0, 0.1, 0.2, 0.3, 0.4, 0.5, 0.6.

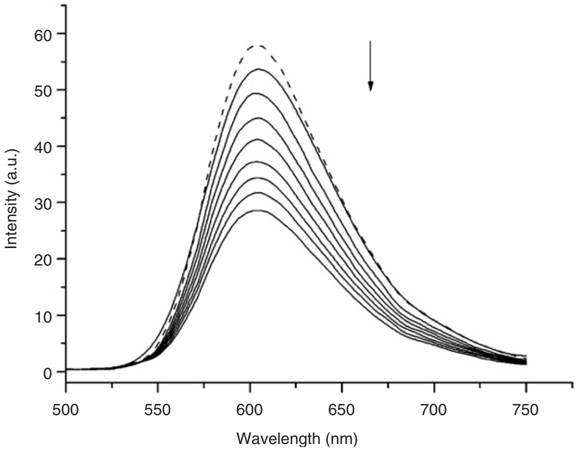

Figure 4. Fluorescence emission spectra (excited at 526 nm) of the EB–CTDNA system (2.5×10^{-5} M EB, 1×10^{-4} M DNA) in the absence (dotted line) and presence (solid line) of **1** (4.0×10^{-3} M, 2 μL per scan).

significant increase in fluorescence emission when bound to DNA and its displacement from DNA results in decrease in fluorescence intensity [27]. Fluorescence titration spectra are shown in figure 4. The emission intensity decreased with increase of concentration of the compound, suggesting that the compound can replace EB from CT-DNA and intercalate into the DNA double helix.

Supplementary material

Crystallographic data for the structural analysis have been deposited with the Cambridge Crystallographic Data Centre, CCDC No. 624084. Copies of this information can be obtained free of charge from The Director, CCDC, 12 Union Road, Cambridge CB2 1EZ, UK (Fax: +44 1223 336033; Email: deposit@ccdc.cam.ac.uk).

Acknowledgements

This work was supported by the National Natural Science Foundation of China (No. 20331020).

References

[1] O. Kahn. *Molecular Magnetism*, VCH Publishers, New York (1993).

[2] E. Coronado, P. Delhae's, D. Gatteschi, J.S. Miller (Eds). *Molecular Magnetism: From Molecular Assemblies to the Devices*, pp. 51–58, Kluwer, Netherlands (1996).

[3] O. Kahn. *Adv. Inorg. Chem.*, **43**, 179 (1996).

[4] O. Kahn. *Angew. Chem., Int. Ed. Engl.*, **24**, 834 (1985).

[5] C.J. Cairns, D.H. Busch. *Coord. Chem.*, **69**, 1 (1986) and references therein.

[6] R. Breslow. *Pure Appl. Chem.*, **54**, 927 (1982).

[7] O. Kahn. *Struct. Bond. (Berlin)*, **68**, 89 (1987).

[8] S. Maheswaran, G. Chastanet, S.J. Teat, T. Mallah, R. Sessoli, W. Wernsdorfer, R.E.P. Winpenny. *Angew. Chem., Int. Ed.*, **44**, 5044 (2005).

[9] C.-F. Wang, J.-L. Zuo, B.M. Bartlett, Y. Song, J.R. Long, X-Z. You. *J. Am. Chem. Soc.*, **128**, 7162 (2006).

[10] J.N. Rebilly, L. Catala, E. Riviere, R. Guillot, W. Wernsdorfer, T. Mallah. *Inorg. Chem*, **44**, 8194 (2005).

[11] Y. Pei, Y. Journaux, O. Kahn. *Inorg. Chem*, **27**, 399 (1988).

[12] J. Ribas, C. Diaz, R. Costa, Y. Journaux, C. Mathonière, O. Kahn, A. Gleizes. *Inorg. Chem*, **29**, 2042 (1990).

[13] R. Vicente, A. Escuer, J. Ribas. *Polyhedron*, **11**, 857 (1992).

[14] J.M. Dominguez-Vera, F. Camara, J.M. Moreno, E. Colacio, H. Stoeckli-Evans. *Inorg. Chem*, **37**, 3046 (1998).

[15] E.-Q. Gao, J.-K. Tang, D.-Z. Liao, Z.-H. Jiang, S.-P. Yan, G.-L. Wang. *Inorg. Chem*, **40**, 3134 (2001).

[16] J. Tercero, C. Diaz, J. Ribas, M. Maestro, J. Mahia, H. Stoeckli-Evans. *Inorg. Chem*, **42**, 3366 (2003).

[17] M.-M. Miao, D.-Z. Liao, Z.-H. Jiang, P. Cheng, G.-L. Wang. *Trans. Met. Chem*, **22**, 330 (1997).

[18] Y. Pei, Y. Journaux, O. Kahn, A. Dei, D. Gatteschi. *J. Chem. Soc., Chem. Commun*, **16**, 1300 (1986).

[19] P. Chaudhuri, M. Winter, B.P.C. Della Védova, P. Fleischhauer, W. Haase, U. Flörke, H.J. Haupt. *Inorg. Chem*, **30**, 4777 (1991).

[20] K. Nonoyama, H. Ojima, M. Nonoyama. *Inorg. Chim. Acta*, **20**, 127 (1976).

[21] G. Haselhorst, S. Stoetzel, A. Strassburger, W. Walz, K. Wieghardt, B. Nuber. *J. Chem. Soc., Dalton Trans*, 83 (1993).

[22] P.W. Selwood. *Magnetochemistry*, p. 78, Interscience, New York (1956).

[23] G.M. Sheldrick. *SHELXS-97 and SHELXL-97, Software for Crystal Structure Analysis*, Siemens Analytical X-Ray Instruments, Inc., Madison, WI (1997).

[24] K. Nakamoto. *Infrared and Raman Spectra of Inorganic and Coordination Compounds*, 5th Edn, Part B, Wiley, New York (1997).

[25] H. Güdel, R.D. Willett, D. Gatteschi, O. Kahn (Eds), in *Magneto-Structural Correlation in Exchange Coupled Systems NATO SAL Series*, p. 241, Reidel, Dordrecht, The Netherlands (1985).

[26] H. Güdel. *Coord. Chem. Rev*, **88**, 69 (1988).

[27] C.V. Kumar, J.K. Barton, N.J. Turro. *J. Am. Chem. Soc*, **107**, 5518 (1985).